Persons using assistive technology may not be able to fully access information in this file. For assistance, e-mail AgingResearchBiobank@imsweb.com. Include the website and filename in your message.

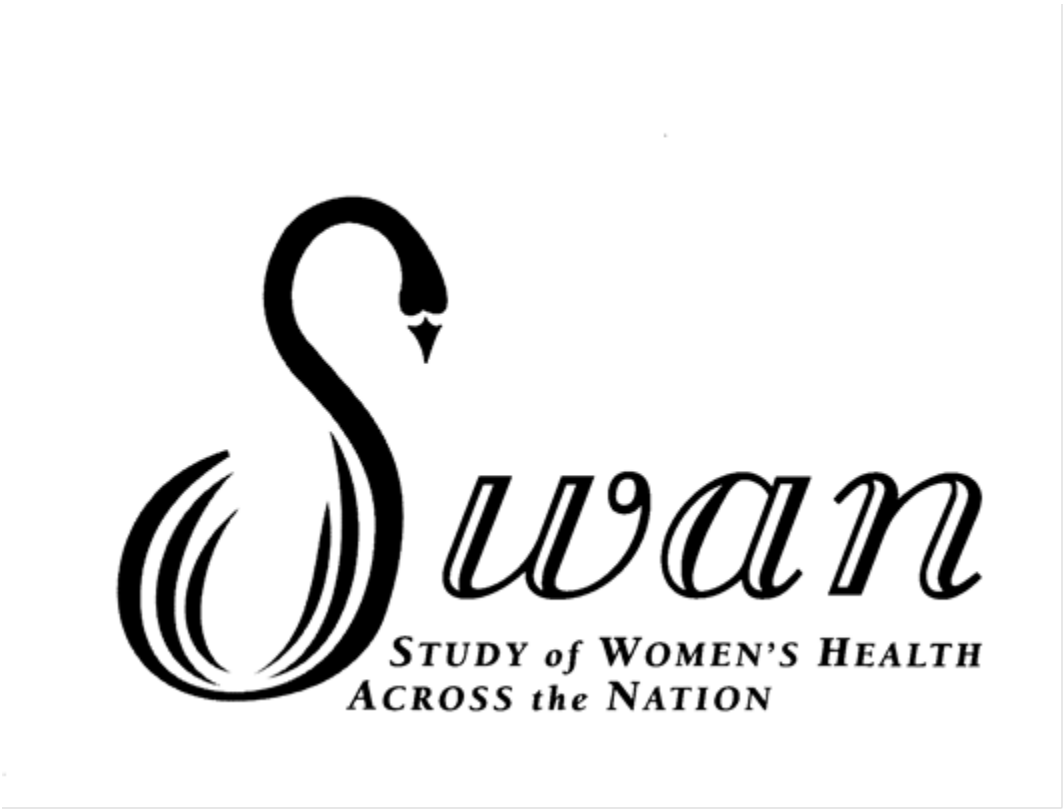

Longitudinal High-Resolution Peripheral Quantitative Computed Tomography (HR-pQCT) Scan Data

Visits 11-13,16, and 17

CODEBOOK

ARCHIVED DATASET 2026

Dataset file niahrpqct2026

PAGE INTENTIONALLY BLANK

DOCUMENTATION FOR THE SWAN LONGITUDINAL HR-PQCT DATASET

This dataset contains all High-Resolution Peripheral Quantitative Computed Tomography (HR-pQCT) Scan Data for the SWAN cohort. It is a longitudinal dataset, meaning that it contains multiple rows of data per ID. SWAN participants who completed HR-pQCT scans at the 1 participating SWAN study site (Massachusetts General Hospital (MGH)) are included in the frozen dataset. This codebook contains detailed information on the technology used to obtain the HR-pQCT measures in this dataset, as well as any other pertinent information for analysis.

Who is included in the public use dataset:

This dataset includes data from 146 participants who completed an HR-pQCT scan at two different visits (Visit 17, along with either Visit 11, 12, 13, or 16), and had data for at least one of the two scans at both.

The assigned participant ID has been replaced with a randomly generated ARCHID in order to protect participant privacy. The baseline interview date is denoted as day 0 and is used as the basis for all other dates. Variables describing the race/ethnicity of participants (RACE) was added from the Screener dataset.

Missing data coding:

Original missing codes (-1: not applicable, -7: refused, -8: don't know, -9: missing) have been recoded to SAS missing codes (.B: not applicable, .D: refused, .C: don't know, and .A: missing).

How the dataset is constructed:

HR-pQCT data were collected in accordance with the manual of procedures. Protocols and procedures followed published guidelines for HR-pQCT data acquisition and analysis [1].

The longitudinal data file contains two rows of data for each participant (one row for the baseline data (V11, 12, 13, or 16) and one row for the follow-up data (V17). The longitudinal sample includes up to 146 postmenopausal women who attended the SWAN HR-pQCT visit 17 (January 2022 – June 2023). The baseline HR-pQCT visit was selected as V12 if available. If V12 was not available, we used HR-pQCT data from V11 or V13, or in one case V16. In total, the data set includes 143 subjects with longitudinal HR-pQCT data at the distal tibia and 130 participants with longitudinal HR-pQCT data at the distal radius. For the tibia, 15 individuals are missing all scan data, whereas n=2 participants are missing just the individual trabecular segmentation (ITS) results. For the radius, 28 participants are missing longitudinal scan data.

HR-pQCT scanning and analysis:

Baseline and follow-up HR-pQCT scans of the distal radius and tibia were obtained at the HRpQCT Imaging Core at Massachusetts General Hospital. Baseline scans were collected at SWAN Visit 11, 12, 13, or 16 using an XTremeCT scanner (SCANCO Medical AG, Brutisellen Switzerland) at the distal radius and tibia. Scan settings included 60 kVp, 900 µA, 100-ms integration time, isotropic voxel size of 82 µm, 110 slices, resulting in images measuring 9.02 mm in axial length. The scans were acquired at a fixed distance of 9.5 and 22.5 mm from the radial and tibial endplates, respectively.

Follow-up scans were collected at SWAN Visit 17 using a second-generation XTremeCT II scanner (SCANCO Medical AG) at the distal radius and tibia using the standard region of interest for the second-generation scanner, 9.0 and 22.0 mm from the radial and tibial endplate, respectively. Scan settings included 68.0 kVp, 1470 µA, 43-ms integration time, isotropic voxel size of 60.7 µm, 168 slices, resulting in images measuring 10.20 mm in axial length. Note the difference (0.5 mm) in offsets from the bone endplate between scanner generations is an adjustment for the longer (1.0 mm) scan region in the 2nd generation scanner, with the result that the centers of the scan regions from each generation of scanner are approximately coincident.

Scans were acquired at the non-dominant radius and tibia, unless there was a previous fracture or metal implant at the site. Longitudinal scans were intended to be acquired at the same site as the baseline scan – if they were not, the longitudinal data were excluded. All scans were reviewed for movement artifact, and scored on a 5-point scale (1 = no movement, 5 = severe movement). Results from scans with movement artifact scores > 3 were excluded from the data set. Quality control was maintained with daily scanning of the manufacturer's QC1 phantom, weekly scanning of the QC2 phantom, and annual preventative maintenance visits for the scanner device.

To enable comparison of the baseline and follow-up scans for longitudinal analyses, follow-up scans were down-scaled to match the voxel size of the baseline scans. The scans were subjected to filtration and segmentation of bone from non-bone, followed by morphologic analysis using Scanco software to derive various parameters, including volumetric bone density of the total, trabecular and cortical regions; trabecular bone volume fraction, thickness, and separation; and cortical thickness and porosity.

These down-scaled follow-up scans were then imported into the database containing the baseline scans, and an automatic matching script was used to define the region of bone common to both scans of each pair. This common region

was identified by matching the total cross-sectional area of slices in each scan in a manner which leverages the natural taper of the radius and tibia cross-section, which becomes smaller as one moves proximally from the distal endplate. Scans with a common overlap region of < 70% were excluded from the longitudinal analyses.

Finite element analysis:

We used microfinite element analysis of the HR-pQCT images to estimate bone stiffness and failure load, simulating axial compression to 1% strain on each radius or tibia using a homogenous Young's modulus of 10 GPa and Poisson's ratio of 0.3. Failure load was estimated using the Pistoia criterion [2]. We employed the μFEA solver provided by the manufacturer (Scanco Medical FE-Software, v 1.19) to solve the finite element models.

The down-scaling of follow-up scans maintains the axial length of the scanned region, such that down-scaled follow-up scans contain 123 slices while the baseline scans which are "native" to the first-generation resolution contain 110 slices. This discrepancy in axial scan length is accounted for in the context of Standard Evaluation and Extended Cortical Evaluation using the cross-sectional area matching, described above, but presents an issue for finite element analysis (FEA) because certain FEA outcomes (specifically compressive stiffness) are linearly dependent on the axial length of the evaluated bone volume. In order to address this, a modified FEA script was utilized to include only the central 110 slices of follow-up scans in the analysis, thus matching the axial length of paired baseline and follow-up scans.

Individual trabecular segmentation (ITS):

We used individual trabecular segmentation, a morphologic analysis technique applied to trabecular bone, to identify individual trabecular rods and plates, as previously described [3]. According to the dimension and orientation of each individual trabeculae, the following variables are computed: plate and rod bone volume fraction (plate bone volume / total volume; rod bone volume / total volume), bone volume fraction along the axial (or longitudinal) axis, tissue fraction of plates and rods (e.g., plate rod volume / bone volume, rod bone volume / bone volume), plate and rod number density, plate and rod thickness, and plate-plate junction density. The validation of ITS methodology against microCT images shows good agreement (r^2 = 0.55 – 0.94) [4].

References:

1. Whittier DE, Boyd SK, Burghardt AJ, Paccou J, Ghasem-Zadeh A, Chapurlat R, Engelke K, Bouxsein ML. Guidelines for the assessment of bone density and microarchitecture in vivo using high-resolution peripheral quantitative computed tomography. *Osteoporos Int.* 2020;31(9):1607-27. Epub 20200526. doi: 10.1007/s00198-020-05438-5. PubMed PMID: 32458029; PMCID: PMC7429313.
2. Pistoia W, van Rietbergen B, Lochmuller EM, Lill CA, Eckstein F, Ruegsegger P. Estimation of distal radius failure load with micro-finite element analysis models based on three-dimensional peripheral quantitative computed tomography images. *Bone.* 2002;30(6):842-8. PubMed PMID: 12052451.
3. Liu XS, Sajda P, Saha PK, Wehrli FW, Bevill G, Keaveny TM, Guo XE. Complete volumetric decomposition of individual trabecular plates and rods and its morphological correlations with anisotropic elastic moduli in human trabecular bone. *J Bone Miner Res.* 2008;23(2):223-35. doi: 10.1359/jbmr.071009. PubMed PMID: 17907921; PMCID: PMC2665696.
4. Dinescu AT, Zhou B, Hu YJ, Agarwal S, Shane E, Guo XE. Individual trabecula segmentation validation in first- and second-generation high-resolution peripheral computed tomography compared to micro-computed tomography in the distal radius and tibia. *JBMR Plus.* 2024;8(3):ziae007. Epub 20240104. doi: 10.1093/jbmrpl/ziae007. PubMed PMID: 38505220; PMCID: PMC10945717.

Variables included in the dataset:

Variable	Description	Codes
ARCHID	Participant ID	
VISIT	Study visit	"00" = Baseline to "17" = Visit 17
RACE	Race/Ethnicity	1 = Black 2 = Chinese/Chinese American 3 = Japanese/Japanese American 4 = White Non-Hispanic 5 = Hispanic
AGE	Participant age, rounded to the nearest 0.1 years.	Numeric
RADSCAN	Indicates if the HR-pQCT scan was conducted on the radius.	0 = No 1 = Yes
TIBSCAN	Indicates if the HR-pQCT scan was conducted on the tibia.	0 = No 1 = Yes

Measured variables: This dataset contains 55 measures taken from the HR-pQCT scan data for both the radius and tibia, for a total of 110 measured variables. All measurements for the radius will have variable names beginning with "R_" and labels beginning with "Radius -", while all measurements for the tibia will have "T_" and "Tibia -".

Variable	Long Name & Units	Description
R_MEASDAY **T_MEASDAY**	Day Scan Collected	The day the HR-pQCT scan was performed.
R_EVALDAY **T_EVALDAY**	Day Scan Evaluated	The day the HR-pQCT scan was evaluated.
R_SCSITE **T_SCSITE**	Scan Site (1=R, 2=L)	Indicates which limb was scanned, either right or left.
R_COMREG **T_COMREG**	Common Region (%)	Region of bone common to the two matched scans, expressed as a percentage of the total scan length.
R_TTAR **T_TTAR**	Total Area (mm^2)	Cross-sectional area of the whole bone.
R_CTARS **T_CTARS**	Cortical Area, from Standard Evaluation (mm^2)	Cross-sectional area of the cortical compartment, calculated without endocortical contours.
R_TBARS **T_TBARS**	Trabecular Area, from Standard Evaluation (mm^2)	Cross-sectional area of the trabecular compartment, calculated without endocortical contours.
R_TTBMD **T_TTBMD**	Total Bone Mineral Density (mg HA/mm^3)	Total bone mineral density within the periosteal surface.
R_CTBMDS **T_CTBMDS**	Cortical Bone Mineral Density, from Standard Evaluation (mg HA/mm^3)	Cortical bone density, calculated without endocortical contours.
R_CTTHS **T_CTTHS**	Cortical Thickness, from Standard Evaluation (mm)	Average thickness of the cortical compartment, calculated without endocortical contours.
R_TBBMD **T_TBBMD**	Trabecular Bone Mineral Density (mg HA/mm^3)	Volumetric bone density of entire trabecular region.
R_TBMTBMD **T_TBMTBMD**	Trabecular Meta Bone Mineral Density (mg HA/mm^3)	Volumetric bone density of the outer portion of the trabecular compartment.
R_TBINBMD **T_TBINBMD**	Trabecular Inner Bone Mineral Density (mg HA/mm^3)	Bone mineral density of the inner region of the trabecular compartment, defined as the central 50% of the trabecular region.
R_TBRMI **T_TBRMI**	Ratio of Meta to Inner BMD	Ratio of the densities of the meta and inner portions of the trabecular compartment.
R_TBBVTVS **T_TBBVTVS**	Trabecular Bone Volume over Total Volume, from Standard Evaluation	Ratio of segmented bone volume to total volume of the trabecular compartment, calculated without endocortical contours; *PREFERRED version of Bone Volume over Total Volume.*
R_TBN **T_TBN**	Trabecular Number (1/mm)	Average number of trabeculae per unit length.
R_TBTH **T_TBTH**	Trabecular Thickness (mm)	Average thickness of trabeculae.

Variable	Long Name & Units	Description
R_TBSP **T_TBSP**	Trabecular Separation (mm)	Average distance between trabeculae.
R_TB1NSD **T_TB1NSD**	Inhomogeneity of Trabecular Network	Measure of inhomogeneity of trabecular network.
R_CTTV **T_CTTV**	Cortical Total Volume (mm^3)	Total volume of the cortical compartment.
R_CTBV **T_CTBV**	Cortical Bone Volume (mm^3)	Volume of segmented bone within the cortical compartment.
R_CTBMDECA **T_CTBMDECA**	Cortical Bone Mineral Density, from Extended Cortical Analysis (ECA) (mg HA/mm^3)	Average bone mineral density within the cortical compartment, calculated using endocortical contours; *PREFERRED form of Cortical Bone Mineral Density.*
R_CTTMD **T_CTTMD**	Cortical Tissue Mineral Density (mg HA/mm^3)	Average density of bone voxels within the cortical compartment, excluding pores.
R_CTARECA **T_CTARECA**	Cortical Area, from Extended Cortical Analysis (ECA) (mm^2)	Measure of the cross-sectional area of the cortical compartment, calculated using endocortical contours; *PREFERRED form of Cortical Area.*
R_TBARECA **T_TBARECA**	Trabecular Area, from Extended Cortical Analysis (ECA) (mm^2)	Measure of the cross-sectional area of the trabecular compartment, calculated using endocortical contours; *PREFERRED form of Trabecular Area.*
R_CTTHECA **T_CTTHECA**	Cortical Thickness, from Extended Cortical Analysis (ECA) (mm)	Average thickness of the cortical compartment, calculated using endocortical contours; *PREFERRED form of Cortical Thickness.*
R_CTPOVM **T_CTPOVM**	Cortical Pore Volume (mm^3)	Total volume of pores within the cortical compartment.
R_CTPOR **T_CTPOR**	Cortical Porosity (%)	Ratio of pore volume relative to the total volume of the cortical compartment, expressed as a percentage.
R_CTPODM **T_CTPODM**	Cortical Pore Diameter (mm)	Average 3D diameter of pore volumes within the cortical compartment.
R_CTPODMSD **T_CTPODMSD**	Cortical Pore Diameter Distribution (mm)	Standard deviation of diameter of pore volumes within the cortical compartment.
R_ECTPER **T_ECTPER**	Endocortical Perimeter (mm)	Length of the endocortical perimeter.
R_FEASTF **T_FEASTF**	Compressive Stiffness (N/mm)	A measure of the bone's ability to resist compression.
R_FEAFL **T_FEAFL**	Failure Load (N)	The force necessary to break the bone in compression.
R_FEAEMOD **T_FEAEMOD**	Apparent Modulus (N/mm^2)	A measure of resistance to compression which is independent of bone size.
R_FEATBD **T_FEATBD**	Load Carried by Trabecular Bone (Distal) (%)	Percent of load carried by trabecular bone at the distal end of the bone.
R_FEACTD **T_FEACTD**	Load Carried by Cortical Bone (Distal) (%)	Percent of load carried by cortical bone at the distal end of the bone.
R_FEATBP **T_FEATBP**	Load Carried by Trabecular Bone (Proximal) (%)	Percent of load carried by trabecular bone at the proximal end of the bone.
R_FEACTP **T_FEACTP**	Load Carried by Cortical Bone (Proximal) (%)	Percent of load carried by cortical bone at the proximal end of the bone.
R_FEATBVM **T_FEATBVM**	Trabecular Von Mises Stress (N/mm^2)	The amount of stress the trabecular compartment can withstand before permanently deforming.
R_FEACTVM **T_FEACTVM**	Cortical Von Mises Stress (N/mm^2)	The amount of stress the cortical compartment can withstand before permanently deforming.
R_TBBVTVI **T_TBBVTVI**	Trabecular Bone Volume over Total Volume, from Individual Trabecular Segmentation (ITS)	Ratio of segmented bone volume to total volume of the trabecular compartment, calculated using endocortical contours; *PREFERRED form of Trabecular Bone Volume over Total Volume.*
R_PLBVTV **T_PLBVTV**	Plate Bone Volume Fraction	The volume of trabecular plates divided by the total bone volume.

Variable	Long Name & Units	Description
R_RODBVTV **T_RODBVTV**	Rod Bone Volume Fraction	The volume of trabecular rods divided by the total bone volume.
R_AXBVTV **T_AXBVTV**	Axial Bone Volume Fraction	The total volume of trabeculae aligned with longitudinal axis divided by the bone volume.
R_PLBVBV **T_PLBVBV**	Plate Tissue Fraction	The total volume of trabecular plates divided by the trabecular bone volume.
R_RODBVBV **T_RODBVBV**	Rod Tissue Fraction	The total volume of trabecular rods divided by the trabecular bone volume.
R_PLN **T_PLN**	Trabecular Plate Number Density (1/mm)	The cubic root of the total number of trabecular plates divided by the bone volume.
R_RODN **T_RODN**	Trabecular Rod Number Density (1/mm)	The cubic root of the total number of trabecular rods divided by the bone volume.
R_PLTH **T_PLTH**	Mean Trabecular Plate Thickness (mm)	The average thickness of trabecular plates.
R_RODTH **T_RODTH**	Mean Trabecular Rod Thickness (mm)	The average diameter of trabecular rods.
R_PLSURF **T_PLSURF**	Mean Trabecular Plate Surface Area (mm^2)	The average surface area of trabecular plates.
R_RODLEN **T_RODLEN**	Mean Trabecular Rod Length (mm)	The average length of trabecular rods.
R_RRJD **T_RRJD**	Rod-Rod Junction Density (1/mm^3)	The total number of junctions between rod and rod divided by the bone volume.
R_RPJD **T_RPJD**	Rod-Plate Junction Density (1/mm^3)	The number of junctions between plate and rod divided by the bone volume.
R_PPJD **T_PPJD**	Plate-Plate Junction Density (1/mm^3)	The total number of junctions between plate and plate divided by the bone volume.